



In vitro skin permeation and rheological evaluation of a transethosomal formulation containing curcumin-tocotrienol combinations for enhanced topical applications

Rajesh Sreedharan Nair, Nashiru Billa & Andrew P. Morris

To cite this article: Rajesh Sreedharan Nair, Nashiru Billa & Andrew P. Morris (19 Aug 2025): In vitro skin permeation and rheological evaluation of a transethosomal formulation containing curcumin-tocotrienol combinations for enhanced topical applications, Journal of Dispersion Science and Technology, DOI: [10.1080/01932691.2025.2542342](https://doi.org/10.1080/01932691.2025.2542342)

To link to this article: <https://doi.org/10.1080/01932691.2025.2542342>



© 2025 The Author(s). Published with license by Taylor & Francis Group, LLC



Published online: 19 Aug 2025.



Submit your article to this journal [↗](#)



Article views: 372



View related articles [↗](#)



View Crossmark data [↗](#)

In vitro skin permeation and rheological evaluation of a transethosomal formulation containing curcumin-tocotrienol combinations for enhanced topical applications

Rajesh Sreedharan Nair^a , Nashiru Billa^b , and Andrew P. Morris^c 

^aFaculty of Science and Engineering, School of Pharmacy, University of Nottingham Malaysia, Semenyih, Malaysia; ^bDepartment of Pharmaceutical Sciences, College of Pharmacy, QU Health, Qatar University, Doha, Qatar; ^cSwansea University Medical School, Swansea University, Swansea, UK

ABSTRACT

Curcumin obtained from *Curcuma longa* has shown anticancer activities against many types of cancers including melanoma. Tocotrienol is a chemosensitizer, and combining curcumin with tocotrienol may potentiate the anti-cancer activity with less harm to healthy cells. However, due to low aqueous solubility and poor skin permeation, topical delivery of these drug combinations is challenging. Therefore, this study aimed to develop a transethosomal formulation containing curcumin and tocotrienol for enhanced topical applications. Zetasizer analysis of the transethosomal formulation (Cu-TRF Ets) showed an average particle size of 129.3 ± 3.0 nm and a zeta potential (ZP) of -87.5 ± 3.0 mV. The scanning transmission electron microscopy (STEM) analysis revealed spherical shapes, with sizes corroborating with Zetasizer results. Fourier transform infrared spectroscopy (FTIR) analysis ensured the compatibility of the drugs within the formulations, while differential scanning calorimetry (DSC) and X-ray diffraction (XRD) analyses confirmed the solid-state nature of curcumin in the formulation. The drug release from the formulations followed a release pattern closely fitting the Korsmeyer-Peppas release model. Permeation studies across synthetic Strat-M[®] membrane and full-thickness human skin demonstrated an enhanced transdermal flux of curcumin and tocotrienol from the Cu-TRF Ets compared to their pure drug solutions ($p < .05$). The rheological evaluation of the transethosome-loaded hydrogel demonstrated a pseudoplastic behavior, and the data approximated the Hershel-Buckley model. The study concludes that co-delivering curcumin and tocotrienol in transethosomal formulations can address the formulation issues associated with both curcumin and tocotrienol, while also enhancing skin permeation.

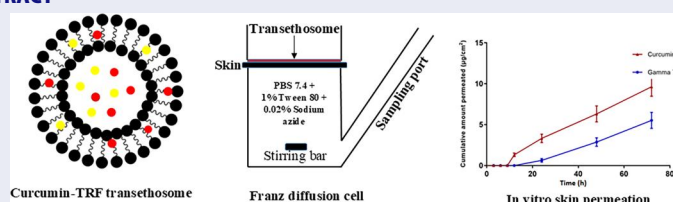
ARTICLE HISTORY

Received 3 January 2025
Accepted 26 July 2025

KEYWORDS

Curcumin; tocotrienol; transethosomes; topical; skin permeation



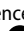
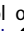
GRAPHICAL ABSTRACT



1. Introduction

Skin cancer is the uncontrolled growth of abnormal cells in the epidermis, the outermost layer of the skin; and in the worst cases, it can extend down to the dermal layer. Melanoma is the least common but most aggressive skin cancer evolving from melanin-producing cells called melanocytes. Melanoma can be treated with surgery, radiation, or chemotherapy.^[1] Despite having several approved medications for the treatment of melanoma, low success rates are attributed to non-adherence due to side effects and multi-drug resistance. Moreover, drug permeation through the

outer rigid stratum corneum (SC) layer of the skin is essential for melanoma treatment *via* topical or transdermal applications. For these reasons, newer safe, efficient, and affordable treatment alternatives are required for melanoma treatment. In the recent past, natural products have widely been studied to evaluate their roles in preventing and treating chronic diseases such as cancer. In this research work, we developed a novel antimelanoma formulation containing two well-known naturally derived anticancer agents, curcumin and tocotrienol, both categorized under generally recognized as safe (GRAS).

CONTACT Rajesh Sreedharan Nair  rajesh.nair@nottingham.edu.my  Faculty of Science and Engineering, School of Pharmacy, University of Nottingham Malaysia, Jalan Broga, 43500 Semenyih, Selangor Darul Ehsan, Malaysia; Andrew P. Morris  a.p.morris@swansea.ac.uk  Swansea University Medical School, Swansea University, Swansea, UK.

© 2025 The Author(s). Published with license by Taylor & Francis Group, LLC

This is an Open Access article distributed under the terms of the Creative Commons Attribution License (<http://creativecommons.org/licenses/by/4.0/>), which permits unrestricted use, distribution, and reproduction in any medium, provided the original work is properly cited. The terms on which this article has been published allow the posting of the Accepted Manuscript in a repository by the author(s) or with their consent.

Curcumin is a phenolic compound obtained from *Curcuma longa* (turmeric) that belongs to the Zingiberaceae family and is indigenous to South and Southeast Asia.^[2] The rhizome part of the plant is most valuable and has been used for centuries as a dietary ingredient and a coloring agent in Asian cuisine. Turmeric has also been traditionally used in many countries as a disinfectant and a household remedy for various skin diseases, insect bites and to promote wound healing.^[3] The therapeutic effects of turmeric are primarily due to curcuminoids, with curcumin being one of the key curcuminoids with innumerable medicinal properties.^[4] Curcumin has been shown to possess anticancer activities against colorectal, hepatic, breast, lung, blood, prostate, and skin cancers, including melanoma.^[5,6] The anticancer properties of curcumin stem from multiple mechanisms whereby the carcinogenesis, angiogenesis, and metastasis phases are all inhibited. Several studies have shown that the cyclooxygenases (COX-1 and COX-2) are involved in tumor proliferation, particularly upregulation of COX-2, resulting in angiogenesis.^[7] Curcumin selectively blocks COX-2, activates the c-Jun N-terminal kinases (JNKs) to cause apoptosis, and inhibits nuclear transcription factor-kappaB (NF- κ B) activation, a protein complex essential for cancer cell survival and resistance.^[8] However, curcumin's bioavailability is hindered by its poor aqueous solubility ($< 1 \mu\text{g/mL}$), rapid gastrointestinal degradation, and hepatic metabolism.^[9] Delivering curcumin through the skin may solve bioavailability issues and enable this compound to be used for treating skin disorders.^[10]

Palm oil contains tocopherols and tocotrienols, with tocotrienols being the most abundant vitamin E.^[11] The tocotrienols are not commonly found in vegetable oils in large quantities, with the main exceptions being rice bran and corn oil.^[12] Tocotrienols have been found to possess antioxidant, neuroprotective, anticancer, and cholesterol-lowering properties that are often not exhibited by the tocopherols.^[13,14] Currently, alpha, gamma, and delta-tocotrienol have emerged as vitamin E molecules with distinct health-promoting benefits than tocopherols.^[15] The polyunsaturated side chain of tocotrienols allows more efficient penetration through the cell membrane, which is said to be the reason for the difference in pharmacological activities between tocopherols and tocotrienols.^[16] Tocotrienols have shown significant anticancer activity against various types of cancers such as skin, breast, lung, brain, prostate, gastrointestinal and genitourinary cancers.^[17] Tocotrienol acts on tumor cells by inhibiting various cellular pathways, including 5-lipoxygenase, COX, NF- κ B, and signal transducer and activator of transcription factor 3 (STAT3).^[18]

Although curcumin and tocotrienol are active against skin cancer, delivering these compounds through the skin is challenging because of their hydrophobicity and poor permeation. For effective skin cancer treatment, the active drugs must pass through the outer epidermal layers and reach the stratum basale layer or dermis. Studies have shown that newer generation lipid carrier systems such as transethosomes,^[19] niosomes,^[20] transferosomes,^[21] and microemulsions^[22] are successful at delivering lipophilic drugs through the skin without disturbing skin's structural integrity.^[23,24] Pham et al.

(2016) report that a tocotrienol nanoemulsion showed enhanced permeation over a tocotrienol-propylene glycol mixture across artificial cellulose ester membranes.^[25] Additionally, in vitro cytotoxicity studies demonstrated that the nanoemulsion formulation was effective against squamous cell carcinoma and human epidermoid carcinoma. Our research group has focused on the topical and transdermal delivery of tocotrienols, and we have previously reported their ability to enhance skin permeation. In particular, we demonstrated that tocotrienol-rich fractions (TRF) derived from crude palm oil significantly increased the skin permeation of moderately lipophilic drugs, such as ibuprofen.^[26] Literature also supports the synergistic anticancer activity of tocotrienols and curcumin on breast cancer cells.^[27] Additionally, tocotrienol is a chemosensitizer and there is the real prospect that delivering curcumin and tocotrienols together in a nanoformulation may reduce the individual dose required and enhance their efficacy in skin cancer therapy. This research describes the development, characterization and in vitro evaluation of deformable transethosomal vesicles containing curcumin and tocotrienol. Transethosomes are advanced nanocarriers that combine the properties of ethosomes and transferosomes, incorporating edge activators (lipid bilayer softening agents) into an ethosomal system.^[28] Unlike conventional vesicular systems such as liposomes, niosomes, or even ethosomes and transferosomes individually, this unique composition enhances superior flexibility, deformability, and enhanced interaction with skin lipids, which collectively facilitate deeper and more efficient penetration through the stratum corneum.^[29,30] Additionally, the skin permeation enhancing properties of TRF would be an added advantage. Taken together, it is hypothesized that the synergistic anticancer effects of tocotrienol and curcumin, combined with the excellent skin permeation capabilities of transethosomes, offer a promising strategy for topical or transdermal applications.

2. Material and methods

2.1. Materials

Curcumin ($>99\%$), curcumin analytical standard, Tween 80 and cholesterol were purchased from Sigma Aldrich, USA. The tocotrienol rich fractions (TRF), and the tocotrienol isomers were provided as a gift sample by ExcelVite Sdn Bhd, Perak, Malaysia. Phosphatidylcholine (25%) of soy lecithin (SPC) was procured from MP Biomedicals, USA. HPLC grade methanol and acetonitrile were purchased from Fisher Scientific, UK.

2.2. Methodology

2.2.1. Formulation of curcumin-TRF transethosomes

Curcumin-TRF transethosomes (Cu-TRF Ets) were prepared by using solvent evaporation and the thin-film hydration method.^[31] In a round-bottom flask, the phospholipid, cholesterol, and tween 80 were dispersed in a chloroform-methanol mixture (2:1). To this mixture, curcumin (5 mg) and TRF (10 mg) were added, and the solvents were

evaporated using a rotary evaporator (Büchi Rotavapor® R-200, Switzerland) at 40 °C and 50 rpm. A film that was deposited on the flask walls was then rehydrated using 10 mL hydroethanolic solution (40%). The rehydrated vesicular mixture was then probe sonicated (Q Sonica,

unentrapped drug. Furthermore, the vesicles were lysed with 10% Triton X and determined the total drug concentration using the same HPLC method. The following equation was used to determine the encapsulation efficiency^[33]:

$$\% \text{ EE} = \frac{\text{The total amount of drug in Cu - TRF Ets} - \text{Drug in the supernatant (Unentrapped drug)}}{\text{The total amount of drug in Cu - TRF Ets}} \quad (1)$$

Newtown, USA) at an amplitude of 20% for 60 seconds to obtain nanoethosomes of the desired size range. The drug-loaded transethosomal formulation was compared with the blank formulation. Additionally, for comparison, ethanol-free vesicles were prepared using the same method, except that the hydroethanolic solution was replaced with phosphate-buffered saline (pH 7.4).

2.2.2. Vesicle size and zeta potential (ZP)

The vesicle size and ZP of the blank and Cu-TRF Ets were determined using a Zetasizer Nano® operated at fixed scattered angle of 173° at 25 °C, with deionized water as the dispersant. The samples were diluted with deionized water (1:3), analyzed at 25 °C. The transethosomal size was recorded as the mean ± standard deviation ($n = 3$).

2.2.3. Scanning transmission electron microscopy (STEM)

Morphological evaluation of the blank and Cu-TRF Ets was performed using a Field Emission Scanning Electron Microscope (Quanta 400 F, FEI, USA). A small amount of ethosome suspension was placed on a copper grid using a micropipette and allowed to dry overnight at 25 °C. The surface characteristics and vesicle size were recorded at 5 kV voltage and 20,000× magnification.

2.2.4. Determination of the encapsulation efficiency (EE)

Prior to this experiment, reverse-phase HPLC methods for the analysis of curcumin and tocotrienol were developed, validated, and reported separately.^[32,33] The analysis was performed using a Hypersil Gold C18 column (250 mm × 4.6 mm) that was maintained at 30 °C. For tocotrienol analysis, the mobile phase consisted of methanol-water (95:05) with a flow rate of 1.1 mL/min, and detection wavelength at 295 nm. Likewise, the mobile phase for the curcumin analysis comprised of a mixture of acetonitrile and 2% v/v acetic acid solution (45:55) with a flow rate of 1.1 mL/min, and detection wavelength of 425 nm. The EE was determined using the ultracentrifugation method reported earlier.^[34] The transethosomal suspension (Cu-TRF Ets) was centrifuged using a benchtop ultracentrifuge (Beckman Coulter, Allegra 64 R) at 25,000 rpm for 45 min and was maintained at 4 °C.^[35] The amount of curcumin and tocotrienol present in the supernatant was determined using the HPLC method, and this was considered to be

2.2.5. Attenuated total reflectance – Fourier transform infrared spectroscopy (ATR-FTIR)

The FTIR spectra of the pure drugs and the formulations were recorded using an ATR-FTIR spectrophotometer (Perkin Elmer, USA). Before starting the experiment, the crystal surface (sample holder) of the ATR-FTIR machine was thoroughly cleaned with acetone to prevent spectral interferences that are likely to arise from contaminants. Following a background scan, a small amount of sample (pure drug/formulation) was placed on the crystal surface, and the spectra were recorded between the scanning frequency 4000–400 cm⁻¹.

2.2.6. Differential scanning calorimetry (DSC)

DSC thermograms of active compounds such as curcumin and tocotrienol, major formulation additives, drug-free transethosomes, and Cu-TRF Ets were recorded using a Q2000 DSC equipped with TA Universal Analysis 2000 software. 10 mg samples were placed in aluminum pans, hermetically sealed with lids, and scanned at a rate of 10 °C/min between 0 and 300 °C.

2.2.7. X-ray diffraction (XRD) analysis

The crystallographic structure of curcumin in the transethosomal formulation was characterized by XRD analysis.^[36] The diffractograms of curcumin, blank formulation, and Cu-TRF Ets were obtained using an “X’pert Pro X-ray diffractometer” with Cu K α as a radiation source operated at 45 kV and 40 mA. The XRD scanning was performed at a scanning rate of 0.02°/step and a step time of 0.5 seconds between 5 and 60°.

2.2.8. Release of curcumin and tocotrienol from Cu-TRF transethosomes

Cryoprotectant (Trehalose Dihydrate 5%) was added to the formulation and frozen at –80 °C overnight. Subsequently, the sample was freeze-dried using a CHRIST® Alpha 2-LD freeze dryer (Osterode am Harz, Germany) at a condenser temperature of –40 °C, and chamber pressure of 0.05 mbar for 48 hours. The freeze-dried nanotransethosomal formulation (200 mg) was dispersed in a 100 mL glass bottle containing release medium and was subjected to a drug release study in a shaker incubator (WiseCube®, Witeg Inc., Germany). The release medium (20 mL) was maintained at

37 °C and consisted of acetate buffer (pH 5) containing 1% w/v tween 80 shaken at 100 rpm. At predetermined intervals, samples (1 mL) were withdrawn and diluted with an equivalent volume of release medium before being centrifuged for 10 min at 25,000 rpm. The released drug present in the supernatant was quantified using the HPLC method outlined in the earlier sections. The drug release profile was generated by plotting the percentage released against time, and the release kinetics were assessed.

2.2.9. Preparation and rheological evaluation of the trans-ethosomes loaded hydrogel

A hydrogel was prepared by dissolving Carbopol® 940 (0.5% w/v) in purified water and allowing it to swell for 24 hours. Triethanolamine was added to adjust the pH to 5.0 and to increase the viscosity.^[37] The optimized formulation (Cu-TRF Ets) was incorporated into the gel by homogeneous mixing using geometric addition. Each gram of hydrogel contains curcumin 0.5 mg and TRF 1.0 mg. The pH of the drug-loaded gel was checked using a Horiba pH meter, and the rheological evaluations were performed using a rheometer (Thermo Haake Rheometer, USA), and data analysis was done using RheoWin Pro software (Version 3.61.00). A 20 mm cone C20/1° with an MP-C60 plate was used for the experiments, and the plate temperature was maintained at 32 °C. The transethosomal gel was evaluated for flow properties, viscosity, and thixotropy. The temperature selection is an important parameter as the thixotropic behavior of a gel can vary largely due to variations in temperature. For this reason, 32 °C was selected as the temperature at which to run the experiment as this approximates the skin surface temperature.

2.2.10. Permeation of Cu-TRF Ets across synthetic Strat-M® membrane and excised full-thickness human skin

The in vitro permeation experiments adopted our previously developed methodology.^[26,34] The ethics approval was obtained from the University Research Ethics Committee before commencing the permeation experiments (Approval No: RS010516). Skin samples were obtained post-abdominoplasty from a local hospital in Kuala Lumpur, Malaysia. The fats and underlying tissues were carefully removed using a scalpel, cut into 3 cm² size, and stored at −20 °C temperature before use. The Franz-type diffusion cell had a donor and receptor volume of approximately 1 mL and 2 mL, respectively, and a permeation area of 0.95 cm². The diffusion cells were placed on a submersible magnetic stirrer block and immersed in a water bath maintained at 37 °C.^[38] The skin or Strat-M® membrane was securely sandwiched between the donor and receptor compartments of the diffusion assembly. The transethosomal formulation (1 gm) was placed on the upper donor side, whereas the receptor side contained PBS and 1% w/v tween 80 supplemented with an antibacterial agent (0.02% w/v sodium azide).^[39] At predetermined time intervals, a 200 µL sample was collected from the receptor chamber using extended-length pipette tips and replaced with an equivalent volume

of receptor fluid. The drug concentrations were determined using the HPLC method reported earlier.^[19]

2.2.11. Stability studies of the formulations

Short term storage stability studies of the blank and drug-loaded formulations were carried out by keeping them at refrigerator conditions (4–8 °C) for 3 months. The particle size, ZP and the drug content were determined at regular intervals.

2.2.12. Statistical analysis

Statistical analyses were performed using GraphPad Prism software (version 9). Data are presented as mean ± standard deviation. The statistical significance between two groups was done using Student's t-test, and multiple group comparison was performed using one-way analysis of variance (ANOVA) followed by post-hoc Tukey-HSD (Honestly Significant Difference), $P < 0.05$ was considered significant.

3. Results and discussion

3.1. Zetasizer and STEM analyses

The Cu-TRF Ets were synthesized using the thin-film hydration technique followed by size reduction. The Zetasizer analysis of the Cu-TRF Ets showed an average size of 129.3 ± 3.0 nm and a ZP of -87.5 ± 3.0 mV. Cu-TRF Ets exhibit a significantly larger vesicle size and higher ZP than the blank formulation (74.4 ± 1.9 nm; -54.0 ± 4.7 mV), possibly due to the incorporation of curcumin and TRF.^[19] Literature suggests that particles less than 300 nm can permeate easily through the SC layer of the skin. Therefore, we attempted to keep the vesicle size as small as possible, and optimized drug-free transethosomes of less than 100 nm were obtained. Ethanol is one of the major components of the ethosomal system and has a significant role in controlling the size, ZP, and skin permeation.^[40] Vesicles synthesized using the same ingredients and method, but without ethanol showed a larger average size of 249 ± 7.5 nm. This clearly indicates that ethanol can decrease the vesicle size, which agrees with previous reports.^[41] Phosphatidylcholines are zwitterionic due to the presence of cationic choline groups and the anionic phosphate and the carbonyl groups.^[42] The ZP of the Cu-TRF Ets (-87.0 ± 4.3) and blank transethosomes (-52.6 ± 3.0) was found to be highly negative, possibly due to the high ethanol percentage, and it was reported that ethanol imparts a net negative charge to the ethosomal system, which could be correlated to the ethanol-free vesicles that provided a low negative ZP (-8.2 ± 0.38 mV). The ethanol is distributed within the lipid bilayers of transethosomes and to the inner aqueous environment. The hydroxyl group of ethanol molecules can stretch to the surface of the vesicles and form hydrogen bonds between ethanol molecules or with water molecules favoring a net negative charge.^[43]

The STEM analysis indicates that both the blank and Cu-TRF Ets demonstrated a spherical shape with smooth edges

(Figure 1a,b). Homogeneously distributed vesicles were observed without aggregation, and these results were in agreement with the low PDI values (<0.25) in the Zetasizer results. Reports suggest that homogeneity and size distribution are better interpreted with a combination of DLS measurements and imaging techniques.^[44] The smaller vesicle size and the spherical shapes of transethosomes can provide significant advantages in skin permeation.^[45]

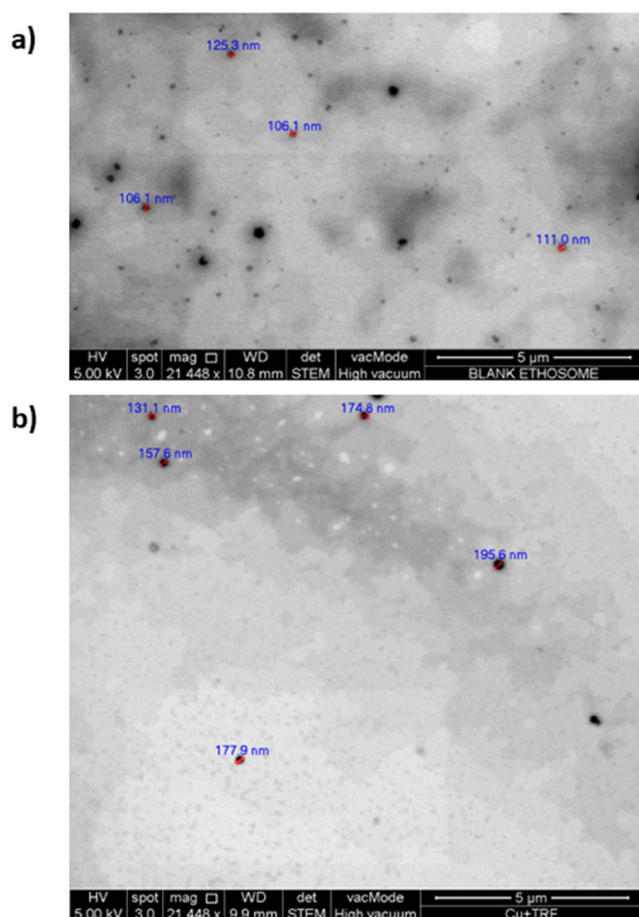


Figure 1. STEM images of (a) blank formulation and (b) Cu-TRF transethosomes at 20,000 \times magnification.

3.2. Encapsulation efficiency

The encapsulation efficiency of Cu-TRF Ets followed a similar pattern to that observed previously for TRF ethosomes and curcumin ethosomes.^[19,33] The curcumin encapsulation in Cu-TRF Ets was $82.0 \pm 1.2\%$, whereas gamma-tocotrienol (gamma-T3) was found to be $65.6 \pm 1.3\%$. Dubey et al. suggest that higher ethanol content enhances drug solubility and, therefore, can accommodate greater drug content in the lipid layer of vesicles.^[46] High EE and optimal vesicle size are vital for the enhanced transdermal delivery of active compounds.

3.3. ATR-FTIR analysis

The compatibility of ethosomal components with curcumin or tocotrienol has been discussed in our recent reports.^[19,33] When assessing the compatibility of curcumin and tocotrienol together in Cu-TRF-Ets, curcumin showed a broad phenolic O-H stretching at 3506.9 cm^{-1} , C=C stretching (1627.3 cm^{-1}), C=O and C=C vibrations (1504.9 cm^{-1}), -olefinic C-H bending vibrations (1426.9 cm^{-1}), and aromatic C-O stretching at 1273.75 cm^{-1} (Figure 2). Tocotrienol had shown prominent peaks of O-H stretching vibration at 3423.4 cm^{-1} , CH₂ stretching (2923.7 cm^{-1} and 2853.8 cm^{-1}), C=C stretch (1723.01 cm^{-1}), C-H bend (1453 cm^{-1}), and 1377.0 cm^{-1} would be a C-C stretch. The characteristics peaks mentioned for curcumin and TRF were visible in the formulated Cu-TRF Ets, suggesting the compatibility of drugs and additives in the formulation.

3.4. DSC analysis

DSC analysis was performed for Cu-TRF Ets, curcumin, TRF, and the other major transethosomal components such as SPC and cholesterol. Figure 3 shows the thermogram of curcumin, TRF, major formulation additives, and transethosomal formulations. An endothermic peak at 150.2°C corresponds to cholesterol melting, whereas the second sharp peak at 179.4°C is attributed to curcumin melting. These sharp peaks disappeared in the drug-free transethosomes and Cu-TRF Ets that were corroborating to other reports.^[36] These results suggest the transition of the crystalline

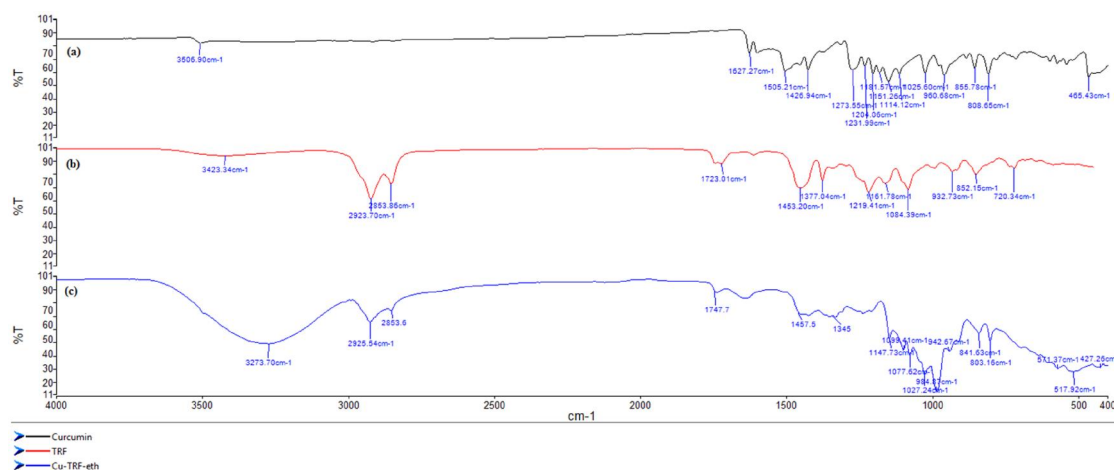


Figure 2. FTIR spectra of curcumin, TRF and Cu-TRF transethosomes.

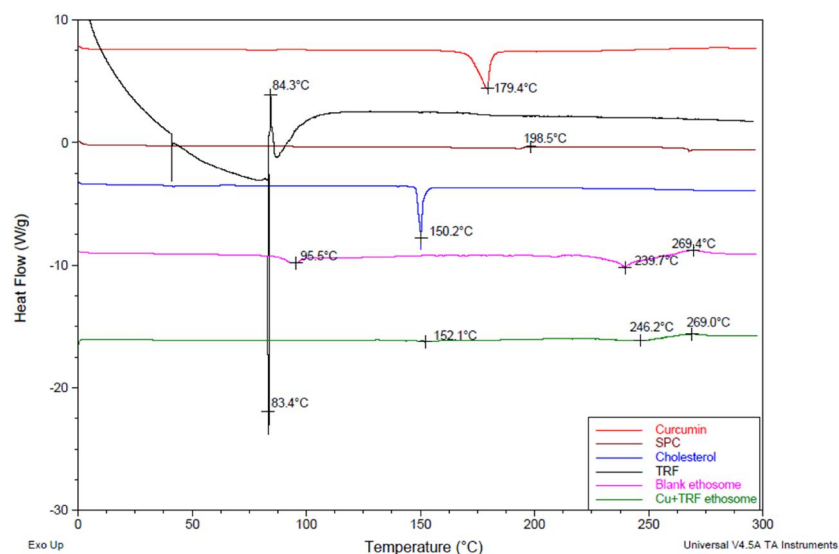


Figure 3. DSC thermogram of pure drugs (curcumin, TRF), formulation additives, blank transethosomes and the CU-TRF transethosomes.

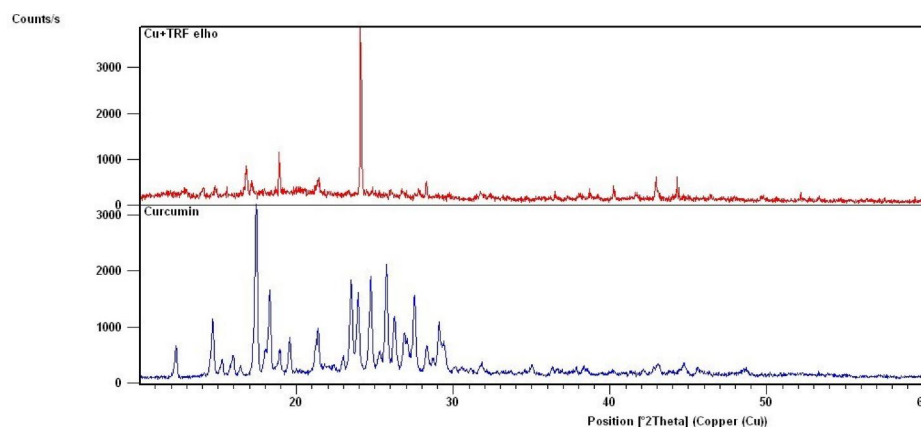


Figure 4. XRD of curcumin and Cu-TRF transethosomes.

arrangement of molecules to a disorderly arranged state, which would have happened during the synthesis. The exothermic peaks seen above 250°C were possibly due to the decomposition of the transethosomal matrix. The DSC analysis supports the successful encapsulation of drugs in the lipid core.

3.5. XRD analysis

Figure 4 shows the XRD diffractogram of curcumin and Cu-TRF Ets. A typical XRD pattern shows the intensity of scattered X-rays from the samples recorded as counts/s. The diffractogram of curcumin showed characteristic peaks between 0° and 30°, attributed to the crystallinity of curcumin. These distinct peaks were either diminished or disappeared in the Cu-TRF Ets diffractograms, possibly due to an amorphous transformation of curcumin from its crystalline state. Many other reports have suggested that the decrease in peak intensity is due to the decreased crystallinity or amorphous nature of the compounds.^[47,48] The change in crystalline characteristics might have occurred due to the intermolecular interactions between drugs and other formulation additives.

3.6. Drug release from Cu-TRF transethosomes

The cumulative drug release from the Cu-TRF Ets was $87.1 \pm 1.7\%$ and $78.5 \pm 1.1\%$, corresponding to the curcumin and gamma-T3, respectively (Figure 5). The drug release followed a continuous release pattern and reached a plateau after 4 hours. The release pattern suggests a controlled drug release with more than 25% of the drug being released in the first 2 hours. Curcumin release was higher than gamma-T3, probably due to their difference in molecular weight. The higher ethanol composition would have enhanced the lipid bilayer's fluidity, which was believed to be the reason for the greater initial drug release.^[49] Drug release from the transethosomal formulations mainly occurs due to the diffusion of drug moieties from the vesicular structure and eventually gets dissolved in the release media. Curcumin and TRF are both poorly water-soluble, so a suitable release medium containing solubilizing agents was necessary to ensure that sink conditions remained. Acetate buffer pH 5.0 containing 1% w/v polysorbate 80 was used as the release medium as it mimics the skin pH, and the addition of the surfactant also enhances the solubility and stability of curcumin and TRF.^[50] The release mechanism was closely fitted to the Korsmeyer-Peppas model with R^2 values of 0.9825

and 0.976 for curcumin and tocotrienol, respectively. Bodade et al. report a similar drug release mechanism from repaglinide-containing transethosomes.^[51] It can be inferred that the enhanced fluidity and erosion of the lipid layer could be the underlying process.

3.7. Rheological evaluation of the transethosomes loaded hydrogel

For Newtonian systems, the shear stress (τ) is directly proportional to the rate of shear ($\dot{\gamma}$), where the viscosity (η) is a constant. Whereas, in the case of non-Newtonian systems, the viscosity is dependent on the shear stress and the shearing rate. Thixotropic behavior is one of the ideal characteristics of topical or transdermal semisolid formulations.^[52] On application, they will change from gel to sol and then regain the gel form. This property offers an easy spreading of the gel on application to the skin, which will remain there for a sufficient duration to exert its therapeutic effect. The rheogram (shear rate vs. viscosity) of the transethosome loaded (Cu-TRF Ets) gel (Figure 6) shows a pseudoplastic (shear thinning) system whereby the viscosity of the gel decreases on increasing shear rate. The gels start to flow above a certain amount of stress which is known as the yield point, and thereafter it behaves like a Newtonian system. The viscosity of the blank and the Cu-TRF Ets gel was found to be 2388 cp and 959.2 cp respectively. This clearly shows a reduction in viscosity on the incorporation of the transethosomes. Several mathematical models have been proposed to

explain the relationship between shear stress and the rate of shear. The rheological data obtained in this study were fitted into different rheological models such as the Bingham model, Hershel-Buckley, and the Casson model.^[53] The Bingham model is a two-factor model that describes the flow of a material based on the yield point and viscosity using the following mathematical expression:

$$\tau = \tau_0 + \eta_p \quad (2)$$

τ_0 is the yield point and η_p is the plastic viscosity

The shearing rate is not accounted for in the Bingham model. Therefore, a modified Bingham model called the Hershel-Buckley model, replacing the viscosity term with the shear rate, consistency index (K), and the flow index (n).

$$\tau = \tau_0 + K\dot{\gamma}^n \quad (3)$$

The Casson model explains the viscoelastic behavior of fluids and is aligned more toward a gradual transition of Newtonian to the yield point, expressed as follows:

$$\tau^{0.5} = \tau_0^{0.5} + \eta_p^{0.5} \cdot \dot{\gamma}^{0.5} \quad (4)$$

Based on the software-generated correlation coefficients (R^2), the data approximated the Hershel-Buckley model (Table 1). This model perfectly describes a non-Newtonian flow of gel where the stress-strain relationship is explained in a non-linear manner.

A hysteresis loop was generated by plotting the shearing stress vs. rate of shear in the ascending and descending order. The thixotropic areas generated for the blank and the Cu-TRF Ets gel were 6444 Pa/s and 1084 Pa/s respectively. It was evident from the data that the blank gel exhibited a higher yield value (51.66 Pa) and thixotropic area compared to the Cu-TRF Ets gel (17.78 Pa). However, both gels were most closely approximated to the Hershel-Buckley model, suggesting that the gel property had been retained even after

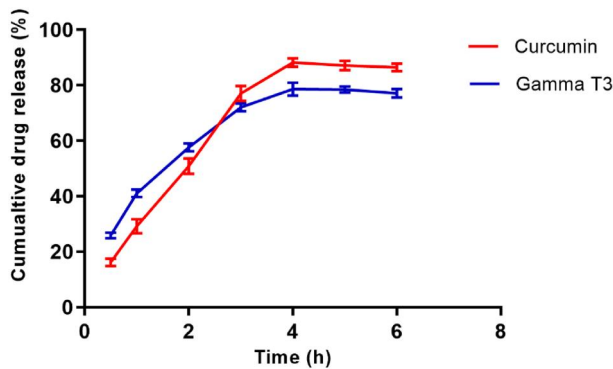


Figure 5. Curcumin and gamma-T3 release from curcumin-TRF transethosomes. Mean \pm SD, $n = 3$.

Table 1. Yield point and the correlation coefficient of the blank and the ethosome loaded (Cu-TRF Ets) gel fitted into various rheological models.

Rheological models	Yield point (τ_0)		Correlation coefficient ' r^2 '	
	Blank Gel Pa	Cu-TRF Ets Gel Pa	Blank Gel	Cu-TRF Ets Gel
Bingham	135.7	35.18	0.9538	0.9520
Casson	98.62	24.67	0.9503	0.9386
Hershel-Buckley	51.66	17.78	0.9680	0.9713

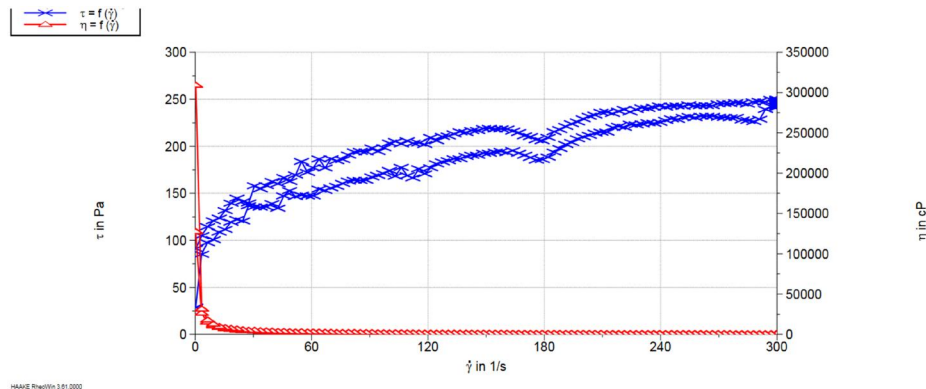


Figure 6. Thixotropic behavior of the gel showing a hysteresis loop between the ascending and descending curves.

incorporating the transethosomes. The reduction in the loop area and the low yield point that was observed in the Cu-TRF Ets gel was probably due to the effect of ethanol on the gel, which might have altered the viscoelastic property of gels. The consistency index obtained for the blank and the Cu-TRF Ets gel was 27.3 and 4.8 respectively, whereas the flow indexes were 0.34 and 0.43, respectively. The K value indicates the consistency of the fluid; therefore, a reduced viscosity was obvious for the Cu-TRF Ets gel due to the dilution that occurred on incorporating transethosomes. A flow index value < 1.0 indicates the pseudoplastic behavior, and a value > 1 suggests the shear thickening or a dilatant behavior.^[54] Hence, these results warrant the pseudoplastic behavior of both the blank and the Cu-TRF formulations, which remain as gels on storage and may go into a sol form on application to the skin.

3.8. In vitro permeation studies of Cu-TRF ets using Strat-M® membrane and excised human skin

Curcumin and tocotrienol permeated through Strat-M® (Figure 7a) in a similar fashion to that previously observed with individual curcumin and tocotrienol ethosomal formulations.^[19,33] The flux values of tocotrienol (gamma-T3) and curcumin from Cu-TRF Ets were $1.93 \pm 0.18 \mu\text{g cm}^{-2} \text{ h}^{-1}$

and $1.23 \pm 0.09 \mu\text{g cm}^{-2} \text{ h}^{-1}$ respectively; this was comparable to the fluxes obtained from the individual formulations. Although TRF as a vehicle has been reported to enhance the permeation of the moderately lipophilic drug ibuprofen (Log P 3.72; MW 206.3 Da),^[26] it did not influence the permeation of curcumin when TRF and curcumin were combined into an transethosomal formulation. This was probably because, as a vehicle, TRF could enhance the permeation of drugs due to its solvent effect. However, when TRF was encapsulated into transethosomes, the permeation was primarily dependent on formulation properties and the drug's physicochemical characteristics. Our formulations contained a high percentage of ethanol and an edge activator tween 80 which could help obtain a soft and flexible vesicle that can easily pass through the skin layers. It is evident from the previous study that the ethosomal formulations showed a significantly enhanced permeation when compared to the control hydroethanolic solution.^[33] This demonstrates unambiguously that ethanol concentration is not the only factor influencing permeation enhancement which agrees with a further study that reported the superior flux from transethosomes compared to an aqueous ethanolic solution or liposomes containing a hydrophobic solution.^[55]

The skin permeation of Cu-TRF Ets through full-thickness human skin (Figure 7b) revealed that curcumin permeation likely exceeded gamma-T3, possibly due to its comparatively low molecular weight (368) and a more favorable log P (3.2). The curcumin permeation would have probably created a momentary channel in the skin that resulted in the faster diffusion of gamma-T3 from Cu-TRF Ets. The cumulative permeation and the flux of curcumin were $9.63 \pm 1.2 \mu\text{g cm}^{-2}$ and $0.16 \pm 0.03 \mu\text{g cm}^{-2} \text{ h}^{-1}$ respectively, whereas the corresponding values for gamma-T3 were $5.51 \pm 0.97 \mu\text{g cm}^{-2}$ and $0.10 \pm 0.02 \mu\text{g cm}^{-2} \text{ h}^{-1}$, and these values were much lower compared to the results obtained using Strat-M®. The significant differences in flux values are due to the structural differences between skin layers and the artificial membrane.

The highly deformable transethosomes can penetrate the SC barrier, fuse with the lipids, and release the encapsulated drugs into deeper skin layers. The SC and other upper epidermal layers are predominantly lipophilic, whereas the lower layers, such as the dermis, are more hydrophilic. Therefore, drugs having a balanced log P (1–4) are ideal for transdermal applications. This was evident from the difference in permeation observed between curcumin and gamma-T3. Curcumin has a lower log P and a lower MW compared to gamma-T3, therefore it can permeate faster than gamma-T3 (log P 8.9) through the lipophilic-hydrophilic regions. The corneocytes of the SC are tightly packed and play a critical role in maintaining the skin's barrier properties and controlling the drug penetration.^[56]

Huq et al. made a comparison of the permeation of hydrophilic and lipophilic compounds across synthetic membranes and human skin. The cumulative permeation reported was in the order of cellulose acetate $>$ Strat-M® $>$ human skin. Although there exists a significant difference between cumulative permeation across human skin and

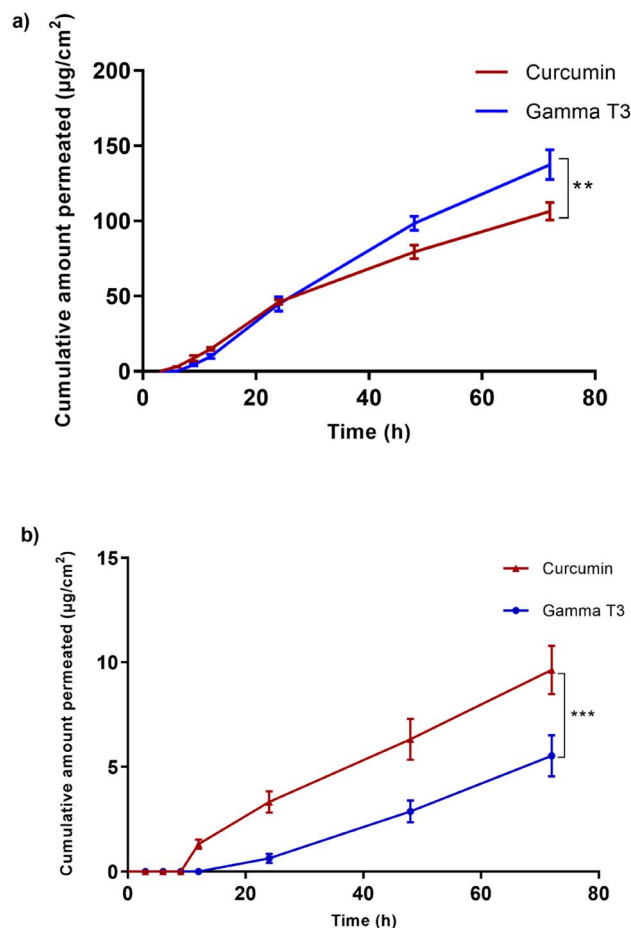


Figure 7. Permeation of curcumin and gamma-T3 from Cu-TRF transethosomes through (a) Strat M® membrane and (b) excised full-thickness human skin. Mean \pm SD, $n = 5$ (***) $p < .001$.

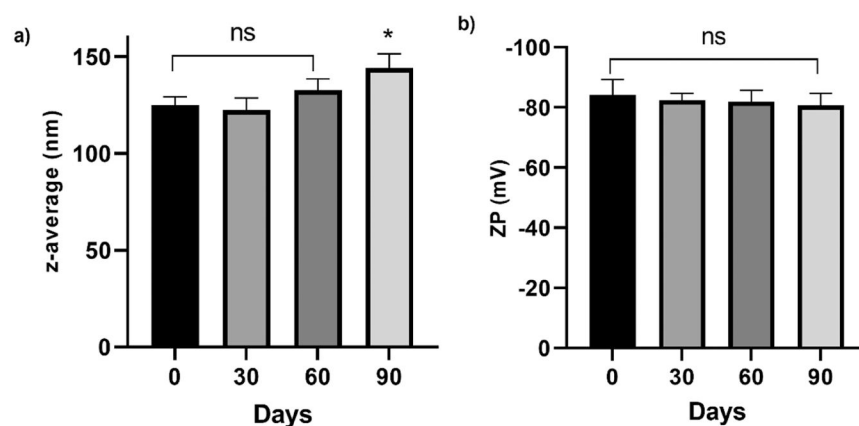


Figure 8. Stability evaluation of Cu-TRF Ets at regular intervals over a 90-day period showing: (a) vesicle size and (b) zeta potential. Data are presented as mean \pm SD, $n = 3$ (* $p < .05$; NS = not significant).

Strat-M[®], the permeation showed a better correlation than other synthetic membranes. The Huq study suggests that Strat-M[®] is a potential alternative to human skin in conducting permeation experiments due to its minimal batch variation and cost-effectiveness.^[57] There are several assumptions about transthesomal skin permeation, and literature reveals a multitude of potential mechanisms. However, most studies suggest that ethanol content plays a significant role as it is a known permeation enhancer and imparts vesicle flexibility that helps diffusibility through the skin layers.^[58,59] Besides, a synergistic mechanism may be involved between ethanol, tween 80 and phospholipids. The phospholipids of transthesosomes may fuse with the skin lipids, altering the lipid transition temperature and increasing fluidity. Additionally, smaller size allows transthesosomes to permeate *via* the transappendageal routes.^[55]

3.9. Stability studies

A short-term stability study of the formulations was performed at 4–8 °C and the z-average, ZP and the EE were determined. The z-average for the blank, and Cu-TRF Ets were observed at 90 days were 79.6 ± 4.0 , and 144.1 ± 7.4 respectively. There were no significant changes between the blanks, but Cu-TRF Ets increased marginally over time ($p < .05$) (Figure 8a). The ZP values showed no significant difference compared to the fresh samples (Figure 8b). A high positive or negative ZP indicate better colloidal stability as oppositely charged colloidal particles will repel each other.^[60,61] Generally, colloids are categorized highly unstable when ZP ranges from 0 to 10 (\pm) mV; moderately stable 10–20 (\pm) mV; relatively stable 20–30 (\pm) mV; >30 highly stable (\pm) mV.^[62] The PDI of all the formulations ranged between 0.23 ± 0.01 and 0.32 ± 0.05 indicating the homogenous size distribution of the formulations. The EE at day 0 was $85.8\% \pm 1.8$ for curcumin and $69.4\% \pm 4.8$ for TRF, while at day 90, it was $80.3\% \pm 3.6$ and $65.1\% \pm 1.8$ respectively for curcumin and TRF. Although the EE fell slightly in all the formulations, but the differences were not significant indicating the short-term stability of the formulations when refrigerated. The particle size and ZP analysis clearly show no aggregation or fusion and thereby warrants

the physical stability of the formulations. Furthermore, the EE analysis showed no major drug loss indicating the chemical stability of the formulations.

4. Conclusion

This study presents a novel approach for co-delivering two safe anticancer agents, curcumin and TRF, incorporated into a transthesosomal formulation, thereby addressing formulation challenges and demonstrating significantly enhanced skin permeation compared to pure curcumin and TRF.^[34,63] Furthermore, to ensure the relevance and reliability of the results, skin permeation was assessed using physiologically relevant models, including Strat-M[®] membranes and excised human skin.^[57] Particle size analysis of the formulation demonstrated that the size range (<200 nm) was ideal for topical application. The FTIR, DSC, and XRD analyses indicate the successful incorporation of curcumin and TRF into the ethosome matrix. The permeation evaluation across Strat-M[®] and the human skin revealed that the transthesosomal formulations could permeate through the skin layers, and the nano-size and the flexibility of transthesosomes may have favored their skin permeation over pure drug solutions ($p < .05$). Future directions include evaluating the anticancer activity of the formulation on melanoma cell lines (SK-MEL-28). To further explore the cytotoxic mechanism, cell cycle analysis and apoptosis assays will be conducted and compared with those of the pure drug solutions. Cytotoxicity will also be assessed on healthy human keratinocytes to determine the selectivity of the formulations between normal and cancer cells.

Disclosure statement

No potential conflict of interest was reported by the author(s).

Funding

The authors received the financial assistance from the Faculty of Science and Engineering, University of Nottingham Malaysia.

ORCID

Rajesh Sreedharan Nair  <http://orcid.org/0000-0002-8540-5044>

Nashiru Billa  <http://orcid.org/0000-0002-8496-1882>

Andrew P. Morris  <http://orcid.org/0000-0002-6315-7553>

References

- [1] Chinembiri, T.; Plessis, L. d.; Gerber, M.; Hamman, J.; Du Plessis, J. Review of Natural Compounds for Potential Skin Cancer Treatment. *Molecules* **2014**, *19*, 11679–11721. DOI: [10.3390/molecules190811679](https://doi.org/10.3390/molecules190811679).
- [2] Urošević, M.; Nikolić, L.; Gajić, I.; Nikolić, V.; Dinić, A.; Miljković, V. Curcumin: Biological Activities and Modern Pharmaceutical Forms. *Antibiotics* **2022**, *11*, 135. DOI: [10.3390/antibiotics11020135](https://doi.org/10.3390/antibiotics11020135).
- [3] Maheshwari, R. K.; Singh, A. K.; Gaddipati, J.; Srimal, R. C. Multiple Biological Activities of Curcumin: A Short Review. *Life Sci.* **2006**, *78*, 2081–2087. DOI: [10.1016/j.lfs.2005.12.007](https://doi.org/10.1016/j.lfs.2005.12.007).
- [4] Fu, Y.-S.; Chen, T.-H.; Weng, L.; Huang, L.; Lai, D.; Weng, C.-F. Pharmacological Properties and Underlying Mechanisms of Curcumin and Prospects in Medicinal Potential. *Biomed. Pharmacother.* **2021**, *141*, 111888. DOI: [10.1016/j.biopha.2021.111888](https://doi.org/10.1016/j.biopha.2021.111888).
- [5] Agrawal, D. K.; Mishra, P. K. Curcumin and Its Analogues: Potential Anticancer Agents. *Med. Res. Rev.* **2010**, *30*, 818–860. DOI: [10.1002/med.20188](https://doi.org/10.1002/med.20188).
- [6] Giordano, A.; Tommonaro, G. Curcumin and Cancer. *Nutrients* **2019**, *11*, 2376. DOI: [10.3390/nu11102376](https://doi.org/10.3390/nu11102376).
- [7] Zoi, V.; Galani, V.; Lianos, G. D.; Voulgaris, S.; Kyritsis, A. P.; Alexiou, G. A. The Role of Curcumin in Cancer Treatment. *Biomedicines* **2021**, *9*, 1086. DOI: [10.3390/biomedicines9091086](https://doi.org/10.3390/biomedicines9091086).
- [8] Vollono, L.; Falconi, M.; Gaziano, R.; Iacovelli, F.; Dika, E.; Terracciano, C.; Bianchi, L.; Campione, E. Potential of Curcumin in Skin Disorders. *Nutrients* **2019**, *11*, 2169. DOI: [10.3390/nu11092169](https://doi.org/10.3390/nu11092169).
- [9] Kumar, S.; Kesharwani, S. S.; Mathur, H.; Tyagi, M.; Bhat, G. J.; Tummala, H. Molecular Complexation of Curcumin with pH Sensitive Cationic Copolymer Enhances the Aqueous Solubility, Stability and Bioavailability of Curcumin. *Eur. J. Pharm. Sci.* **2016**, *82*, 86–96. DOI: [10.1016/j.ejps.2015.11.010](https://doi.org/10.1016/j.ejps.2015.11.010).
- [10] Peram, M. R.; Jalalpure, S.; Kumbhar, V.; Patil, S.; Joshi, S.; Bhat, K.; Diwan, P. Factorial Design Based Curcumin Ethosomal Nanocarriers for the Skin Cancer Delivery: In Vitro Evaluation. *J. Liposome Res.* **2019**, *29*, 291–311. DOI: [10.1080/08982104.2018.1556292](https://doi.org/10.1080/08982104.2018.1556292).
- [11] Looi, A. D.; Palanisamy, U. D.; Moorthy, M.; Radhakrishnan, A. K. Health Benefits of Palm Tocotrienol-Rich Fraction: A Systematic Review of Randomized Controlled Trials. *Nutr. Rev.* **2025**, *83*, 307–328. DOI: [10.1093/nutrit/nuae061](https://doi.org/10.1093/nutrit/nuae061).
- [12] Ranasinghe, R.; Mathai, M.; Zulli, A. Revisiting the Therapeutic Potential of Tocotrienol. *Biofactors* **2022**, *48*, 813–856. DOI: [10.1002/biof.1873](https://doi.org/10.1002/biof.1873).
- [13] Zainal, Z.; Khaza'ai, H.; Kutty Radhakrishnan, A.; Chang, S. K. Therapeutic Potential of Palm Oil Vitamin E-Derived Tocotrienols in Inflammation and Chronic Diseases: Evidence from Preclinical and Clinical Studies. *Food Res. Int.* **2022**, *156*, 111175. DOI: [10.1016/j.foodres.2022.111175](https://doi.org/10.1016/j.foodres.2022.111175).
- [14] Mathew, A. M.; Bhuvanendran, S.; Nair, R. S.; K.R., A. Exploring the anti-Inflammatory Activities, Mechanism of Action and Prospective Drug Delivery Systems of Tocotrienol to Target Neurodegenerative Diseases. *F1000Res.* **2023**, *12*, 338. DOI: [10.12688/f1000research.131863.1](https://doi.org/10.12688/f1000research.131863.1).
- [15] Sen, C. K.; Khanna, S.; Roy, S. Tocotrienols: Vitamin E beyond Tocopherols. *Life Sci.* **2006**, *78*, 2088–2098. DOI: [10.1016/j.lfs.2005.12.001](https://doi.org/10.1016/j.lfs.2005.12.001).
- [16] Mutalib, M. S. A.; Khaza'ai, H.; Wahle, K. W. J. Palm-Tocotrienol Rich Fraction (TRF) Is a More Effective Inhibitor of LDL Oxidation and Endothelial Cell Lipid Peroxidation Than α -Tocopherol In Vitro. *Food Res. Int.* **2003**, *36*, 405–413. DOI: [10.1016/S0963-9969\(02\)00173-4](https://doi.org/10.1016/S0963-9969(02)00173-4).
- [17] Aggarwal, V.; Kashyap, D.; Sak, K.; Tuli, H. S.; Jain, A.; Chaudhary, A.; Garg, V. K.; Sethi, G.; Yerer, M. B. Molecular Mechanisms of Action of Tocotrienols in Cancer: Recent Trends and Advancements. *Int. J. Mol. Sci.* **2019**, *20*, 656. DOI: [10.3390/ijms20030656](https://doi.org/10.3390/ijms20030656).
- [18] Sailo, B. L.; Banik, K.; Padmavathi, G.; Javadi, M.; Bordoloi, D.; Kunnumakkara, A. B. Tocotrienols: The Promising Analogues of Vitamin E for Cancer Therapeutics. *Pharmacol. Res.* **2018**, *130*, 259–272. DOI: [10.1016/j.phrs.2018.02.017](https://doi.org/10.1016/j.phrs.2018.02.017).
- [19] Nair, R. S.; Billa, N.; Leong, C.-O.; Morris, A. P. An Evaluation of Tocotrienol Ethosomes for Transdermal Delivery Using Strat-M® Membrane and Excised Human Skin. *Pharm. Dev. Technol.* **2021**, *26*, 243–251. DOI: [10.1080/10837450.2020.1860087](https://doi.org/10.1080/10837450.2020.1860087).
- [20] Shah, J.; Nair, A. B.; Shah, H.; Jacob, S.; Shehata, T. M.; Morsy, M. A. Enhancement in Antinociceptive and Anti-Inflammatory Effects of Tramadol by Transdermal Proniosome Gel. *Asian J. Pharm. Sci.* **2020**, *15*, 786–796. DOI: [10.1016/j.ajps.2019.05.001](https://doi.org/10.1016/j.ajps.2019.05.001).
- [21] Das, B.; Sen, S. O.; Maji, R.; Nayak, A. K.; Sen, K. K. Transfersomal Gel for Transdermal Delivery of Risperidone: Formulation Optimization and Ex Vivo Permeation. *J. Drug Deliv. Sci. Technol.* **2017**, *38*, 59–71. DOI: [10.1016/j.jddst.2017.01.006](https://doi.org/10.1016/j.jddst.2017.01.006).
- [22] Sha, K.; Ma, Q.; Veroniaina, H.; Qi, X.; Qin, J.; Wu, Z. Formulation Optimization of Solid Self-Microemulsifying Pellets for Enhanced Oral Bioavailability of Curcumin. *Pharm. Dev. Technol.* **2021**, *26*, 549–558. DOI: [10.1080/10837450.2021.1899203](https://doi.org/10.1080/10837450.2021.1899203).
- [23] El Maghraby, G. M.; Williams, A. C. Vesicular Systems for Delivering Conventional Small Organic Molecules and Larger Macromolecules to and through Human Skin. *Expert Opin. Drug Deliv.* **2009**, *6*, 149–163. DOI: [10.1517/17425240802691059](https://doi.org/10.1517/17425240802691059).
- [24] Manickam, B.; Sreedharan, R.; Chidambaram, K. Drug/Vehicle Impacts and Formulation Centered Stratagems for Enhanced Transdermal Drug Permeation, Controlled Release and Safety: Unparalleled Past and Recent Innovations-an Overview. *CDTH.* **2019**, *14*, 192–209. DOI: [10.2174/1574885514666190212113754](https://doi.org/10.2174/1574885514666190212113754).
- [25] Pham, J.; Nayel, A.; Hoang, C.; Elbayoumi, T. Enhanced Effectiveness of Tocotrienol-Based Nano-Emulsified System for Topical Delivery against Skin Carcinomas. *Drug Deliv.* **2016**, *23*, 1514–1524. DOI: [10.3109/10717544.2014.966925](https://doi.org/10.3109/10717544.2014.966925).
- [26] Singh, I.; Nair, R. S.; Gan, S.; Cheong, V.; Morris, A. An Evaluation of Crude Palm Oil (CPO) and Tocotrienol Rich Fraction (TRF) of Palm Oil as Percutaneous Permeation Enhancers Using Full-Thickness Human Skin. *Pharm. Dev. Technol.* **2019**, *24*, 448–454. DOI: [10.1080/10837450.2018.1509347](https://doi.org/10.1080/10837450.2018.1509347).
- [27] Nesaretnam, K.; Selvaduray, K. R. Synergistic Effect of Tocotrienols and Curcumin. <http://palmoilis.mpob.gov.my/publications/TOT/TT585.pdf> (2015, accessed January 10, 2020).
- [28] Seenivasan, R.; Halagali, P.; Nayak, D.; Tippavajhala, V. K. Transethosomes: A Comprehensive Review of Ultra-Deformable Vesicular Systems for Enhanced Transdermal Drug Delivery. *AAPS PharmSciTech* **2025**, *26*, 41. DOI: [10.1208/s12249-024-03035-x](https://doi.org/10.1208/s12249-024-03035-x).
- [29] Chen, Z.; Li, B.; Liu, T.; Wang, X.; Zhu, Y.; Wang, L.; Wang, X.; Niu, X.; Xiao, Y.; Sun, Q. Evaluation of Paeonol-Loaded Transethosomes as Transdermal Delivery Carriers. *Eur. J. Pharm. Sci.* **2017**, *99*, 240–245. DOI: [10.1016/j.ejps.2016.12.026](https://doi.org/10.1016/j.ejps.2016.12.026).
- [30] Raj, A.; Dua, K.; Nair, R. S.; Sarath Chandran, C.; Alex, A. T. Transethosome: An Ultra-Deformable Ethanolic Vesicle for Enhanced Transdermal Drug Delivery. *Chem. Phys. Lipids* **2023**, *255*, 105315. DOI: [10.1016/j.chemphyslip.2023.105315](https://doi.org/10.1016/j.chemphyslip.2023.105315).
- [31] Toutou, E.; Dayan, N.; Bergelson, L.; Godin, B.; Eliaz, M. Ethosomes—Novel Vesicular Carriers for Enhanced Delivery: Characterization and Skin Penetration Properties. *J. Control.*

- Release* **2000**, 65, 403–418. DOI: [10.1016/S0168-3659\(99\)00222-9](https://doi.org/10.1016/S0168-3659(99)00222-9).
- [32] Nair, R. S.; Billa, N.; Morris, A. A Validated Reverse-Phase High Performance Liquid Chromatography (RP-HPLC) Method for the Quantification of Gamma-Tocotrienol in Tocotrienol Rich Fractions of Crude Palm Oil. *CNF* **2022**, 18, 75–81. DOI: [10.2174/1573401317666210803155717](https://doi.org/10.2174/1573401317666210803155717).
- [33] Nair, R. S.; Billa, N.; Mooi, L. Y.; Morris, A. P. Characterization and Ex Vivo Evaluation of Curcumin Nanoethosomes for Melanoma Treatment. *Pharm. Dev. Technol.* **2022**, 27, 72–82. DOI: [10.1080/10837450.2021.2023568](https://doi.org/10.1080/10837450.2021.2023568).
- [34] Nair, R. S.; Morris, A.; Billa, N.; Leong, C.-O. An Evaluation of Curcumin-Encapsulated Chitosan Nanoparticles for Transdermal Delivery. *AAPS PharmSciTech* **2019**, 20, 69. DOI: [10.1208/s12249-018-1279-6](https://doi.org/10.1208/s12249-018-1279-6).
- [35] Abd El-Alim, S. H.; Kassem, A. A.; Basha, M.; Salama, A. Comparative Study of Liposomes, Ethosomes and Transfersomes as Carriers for Enhancing the Transdermal Delivery of Diflunisal: In Vitro and In Vivo Evaluation. *Int. J. Pharm.* **2019**, 563, 293–303. DOI: [10.1016/j.ijpharm.2019.04.001](https://doi.org/10.1016/j.ijpharm.2019.04.001).
- [36] Wan, S.; Sun, Y.; Qi, X.; Tan, F. Improved Bioavailability of Poorly Water-Soluble Drug Curcumin in Cellulose Acetate Solid Dispersion. *AAPS PharmSciTech* **2012**, 13, 159–166. DOI: [10.1208/s12249-011-9732-9](https://doi.org/10.1208/s12249-011-9732-9).
- [37] Sreedharan Nair, R.; Rahman, H.; Kong, M. X.; Tan, X. Y.; Chen, K. Y.; Shanmugham, S. Development and Rheological Evaluation of DEET (N,N-Diethyl-3-Methylbenzamide) Microparticles Loaded Hydrogel For Topical Application. *Turk. J. Pharm. Sci.* **2021**, 18, 352–359. DOI: [10.4274/tjps.galenos.2020.88725](https://doi.org/10.4274/tjps.galenos.2020.88725).
- [38] Sreedharan Nair, R.; Nair, S. Permeation Studies of Captopril Transdermal Films Through Human Cadaver Skin. *Curr. Drug Deliv.* **2015**, 12, 517–523. DOI: [10.2174/1567201812666150212124508](https://doi.org/10.2174/1567201812666150212124508).
- [39] Nair, R. S.; Billa, A.; Morris, P. Optimizing In Vitro Skin Permeation Studies to Obtain Meaningful Data in Topical and Transdermal Drug Delivery. *AAPS PharmSciTech* **2025**, 26, 147. DOI: [10.1208/s12249-025-03143-2](https://doi.org/10.1208/s12249-025-03143-2).
- [40] Dave, V.; Kumar, D.; Lewis, S.; Paliwal, S. Ethosome for Enhanced Transdermal Drug Delivery of Aceclofenac. *Int. J. Drug Deliv.* **2010**, 2, 81–92. DOI: [10.5138/ijdd.2010.0975.0215.02016](https://doi.org/10.5138/ijdd.2010.0975.0215.02016).
- [41] Zhao, Y.-Z.; Lu, C.-T.; Zhang, Y.; Xiao, J.; Zhao, Y.-P.; Tian, J.-L.; Xu, Y.-Y.; Feng, Z.-G.; Xu, C.-Y. Selection of High Efficient Transdermal Lipid Vesicle for Curcumin Skin Delivery. *Int. J. Pharm.* **2013**, 454, 302–309. DOI: [10.1016/j.ijpharm.2013.06.052](https://doi.org/10.1016/j.ijpharm.2013.06.052).
- [42] Bhagavan, N. V.; Ha, C.-E. Chapter 17 - Lipids II: Phospholipids, Glycosphingolipids, and Cholesterol. In *Essentials of Medical Biochemistry*, 2nd ed.; Bhagavan, N. V., Ha, C.-E., Eds. Academic Press: San Diego, CA, **2015**; pp 299–320.
- [43] Zhai, Y.; Xu, R.; Wang, Y.; Liu, J.; Wang, Z.; Zhai, G. Ethosomes for Skin Delivery of Ropivacaine: Preparation, Characterization and Ex Vivo Penetration Properties. *J. Liposome Res.* **2015**, 25, 316–324. DOI: [10.3109/08982104.2014.999686](https://doi.org/10.3109/08982104.2014.999686).
- [44] Eaton, P.; Quaresma, P.; Soares, C.; Neves, C.; de Almeida, M. P.; Pereira, E.; West, P. A Direct Comparison of Experimental Methods to Measure Dimensions of Synthetic Nanoparticles. *Ultramicroscopy* **2017**, 182, 179–190. DOI: [10.1016/j.ultramicro.2017.07.001](https://doi.org/10.1016/j.ultramicro.2017.07.001).
- [45] Zeb, A.; Qureshi, O. S.; Kim, H.-S.; Cha, J.-H.; Kim, H.-S.; Kim, J.-K. Improved Skin Permeation of Methotrexate via Nanosized Ultradeformable Liposomes. *Int. J. Nanomed.* **2016**, 11, 3813–3824. DOI: [10.2147/IJN.S109565](https://doi.org/10.2147/IJN.S109565).
- [46] Dubey, V.; Mishra, D.; Dutta, T.; Nahar, M.; Saraf, D.; Jain, N. Dermal and Transdermal Delivery of an Anti-Psoriatic Agent via Ethanolic Liposomes. *J. Control. Release* **2007**, 123, 148–154. DOI: [10.1016/j.jconrel.2007.08.005](https://doi.org/10.1016/j.jconrel.2007.08.005).
- [47] Chereddy, K. K.; Coco, R.; Memvanga, P. B.; Ucar, B.; Des Rieux, A.; Vandermeulen, G.; Pr  at, V. Combined Effect of PLGA and Curcumin on Wound Healing Activity. *J. Control. Release* **2013**, 171, 208–215. DOI: [10.1016/j.jconrel.2013.07.015](https://doi.org/10.1016/j.jconrel.2013.07.015).
- [48] Mahmood, S.; Mandal, U. K.; Chatterjee, B. Transdermal Delivery of Raloxifene HCl via Ethosomal System: Formulation, Advanced Characterizations and Pharmacokinetic Evaluation. *Int. J. Pharm.* **2018**, 542, 36–46. DOI: [10.1016/j.ijpharm.2018.02.044](https://doi.org/10.1016/j.ijpharm.2018.02.044).
- [49] Chourasia, M. K.; Kang, L.; Chan, S. Y. Nanosized Ethosomes Bearing Ketoprofen for Improved Transdermal Delivery. *Results Pharma Sci.* **2011**, 1, 60–67. DOI: [10.1016/j.rinphs.2011.10.002](https://doi.org/10.1016/j.rinphs.2011.10.002).
- [50] Doaa Nabih, M.; Sanjay, R. M.; Lijia, W.; Abd-Elgawad Helmy, A.-E.; Osama Abd-Elazeem, S.; Marwa Salah, E.-D.; Monica, M. J. Water-Soluble Complex of Curcumin with Cyclodextrins: Enhanced Physical Properties for Ocular Drug Delivery. *Curr. Drug Deliv.* **2017**, 14, 875–886. DOI: [10.2174/1567201813666160808111209](https://doi.org/10.2174/1567201813666160808111209).
- [51] Bodade, S. S.; Shaikh, K. S.; Kamble, M. S.; Chaudhari, P. D. A Study on Ethosomes as Mode for Transdermal Delivery of an Antidiabetic Drug. *Drug Deliv.* **2013**, 20, 40–46. DOI: [10.3109/10717544.2012.752420](https://doi.org/10.3109/10717544.2012.752420).
- [52] Berdey, I. O. V. Rheological Properties of Emulgel Formulations Based on Different Gelling Agent. *Pharm. Innov.* **2016**, 5, 76–79.
- [53] Ortan, A.; Parvu, M. C. D.; Ghica, L. V.; Popescu, M.; Ionita, L. Rheological Study of a Liposomal Hydrogel Based on Carbopol. *Roman. Biotechnol. Lett.* **2011**, 16, 47–54.
- [54] Seyssiecq, I.; Ferrasse, J.-H.; Roche, N. State-of-the-Art: Rheological Characterisation of Wastewater Treatment Sludge. *Biochem. Eng. J.* **2003**, 16, 41–56. DOI: [10.1016/S1369-703X\(03\)00021-4](https://doi.org/10.1016/S1369-703X(03)00021-4).
- [55] Yang, L.; Wu, L.; Wu, D.; Shi, D.; Wang, T.; Zhu, X. Mechanism of Transdermal Permeation Promotion of Lipophilic Drugs by Ethosomes. *Int. J. Nanomed.* **2017**, 12, 3357–3364. DOI: [10.2147/IJN.S134708](https://doi.org/10.2147/IJN.S134708).
- [56] Sapra, B.; Jindal, M.; Tiwary, A. K. Tight Junctions in Skin: New Perspectives. *Ther. Deliv.* **2012**, 3, 1297–1327. DOI: [10.4155/tde.12.118](https://doi.org/10.4155/tde.12.118).
- [57] Haq, A.; Goodyear, B.; Ameen, D.; Joshi, V.; Michniak-Kohn, B. Strat-M[®] Synthetic Membrane: Permeability Comparison to Human Cadaver Skin. *Int. J. Pharm.* **2018**, 547, 432–437. DOI: [10.1016/j.ijpharm.2018.06.012](https://doi.org/10.1016/j.ijpharm.2018.06.012).
- [58] Verma, P.; Pathak, K. Therapeutic and Cosmeceutical Potential of Ethosomes: An Overview. *J. Adv. Pharm. Technol. Res.* **2010**, 1, 274–282. DOI: [10.4103/0110-5558.72415](https://doi.org/10.4103/0110-5558.72415).
- [59] Pandey, V.; Golhani, D.; Shukla, R. Ethosomes: Versatile Vesicular Carriers for Efficient Transdermal Delivery of Therapeutic Agents. *Drug Deliv.* **2015**, 22, 988–1002. DOI: [10.3109/10717544.2014.889777](https://doi.org/10.3109/10717544.2014.889777).
- [60] Sguizzato, M.; Ferrara, F.; Hallan, S. S.; Baldisserotto, A.; Drechsler, M.; Malatesta, M.; Costanzo, M.; Cortesi, R.; Puglia, C.; Valacchi, G.; Esposito, E. Ethosomes and Transethosomes for Mangiferin Transdermal Delivery. *Antioxidants* **2021**, 10, 768. DOI: [10.3390/antiox10050768](https://doi.org/10.3390/antiox10050768).
- [61] Mishra, K. K.; Kaur, C. D.; Gupta, A. Development of Itraconazole Loaded Ultra-Deformable Transethosomes Containing Oleic-Acid for Effective Treatment of Dermatophytosis: Box-Behnken Design, Ex-Vivo and in-Vivo Studies. *J. Drug Deliv. Sci. Technol.* **2022**, 67, 102998. DOI: [10.1016/j.jddst.2021.102998](https://doi.org/10.1016/j.jddst.2021.102998).
- [62] Bhattacharjee, S. DLS and Zeta Potential – What They Are and What They Are Not? *J. Control. Release* **2016**, 235, 337–351. DOI: [10.1016/j.jconrel.2016.06.017](https://doi.org/10.1016/j.jconrel.2016.06.017).
- [63] Sri, P.; Adimoolam, S.; Mahmud, A. Percutaneous Absorption of Triacylglycerols (TAGS), Tocols and Carotenoids: Comparison Studies of Crude and Refined Palm Oil. *Malays. J. Pharm. Sci.* **2013**, 11, 33–48.